Molecular Cell, Vol. 20, 277–287, October 28, 2005, Copyright ©2005 by Elsevier Inc. DOI 10.1016/j.molcel.2005.09.007

Folding of CFTR Is Predominantly Cotranslational

Bertrand Kleizen,[1,3] Thijs van Vlijmen,[1,4] Hugo R. de Jonge,[2] and Ineke Braakman[1,*]
[1]Cellular Protein Chemistry
Department of Chemistry
Utrecht University
Padualaan 8
3584 CH Utrecht
The Netherlands
[2]Department of Biochemistry
Erasmus University Medical Center
Rotterdam
The Netherlands

Summary

The folding process for newly synthesized, multispanning membrane proteins in the endoplasmic reticulum (ER) is largely unknown. Here, we describe early folding events of the cystic fibrosis transmembrane conductance regulator (CFTR), a member of the ABC-transporter family. In vitro translation of CFTR in the presence of semipermeabilized cells allowed us to investigate this protein during nascent chain elongation. We found that CFTR folds mostly during synthesis as determined by protease susceptibility. C-terminally truncated constructs showed that individual CFTR domains formed well-defined structures independent of C-terminal parts. We conclude that the multidomain protein CFTR folds mostly cotranslationally, domain by domain.

Introduction

The endoplasmic reticulum (ER) is a highly versatile organelle that functions as a folding factory where many proteins attain their native structure (Ellgaard and Helenius, 2003). Protein folding starts during translation and translocation of nascent polypeptide chains and proceeds for minutes to hours after synthesis. It has been characterized for several disulfide bond-containing soluble and single-spanning membrane proteins. Thyroglobulin (Kim et al., 1992), the LDL-receptor (Jansens et al., 2002), and various viral glycoproteins (Morrison et al., 1987) are examples of proteins that undergo extensive posttranslational folding. Influenza virus hemagglutinin (HA) (Chen and Helenius, 2000) starts folding during synthesis and continues after translation termination. Several other proteins such as Immunoglobulin heavy chain G (Bergman and Kuehl, 1979) and ER-targeted Semliki Forest virus capsid protease (Kowarik et al., 2002) were found to fold completely cotranslationally. A combination of intrinsic protein features and cellular assistance by chaperones may determine whether folding is completed at the moment of chain termination or not.

Large integral membrane proteins constitute an important class of proteins that represent ~20%–30% of our genome (Wallin and von Heijne, 1998). Compared to soluble and single-spanning membrane proteins that enter the ER lumen, these large proteins require more interplay between the ribosome and the Sec61 translocon pore (Alder and Johnson, 2004; Clemons et al., 2004). Next to the many transmembrane segments that need to be translated and inserted into the membrane, the soluble parts located in both the ER lumen and the cytosol must be synthesized and folded. The question is whether transmembrane segments and cytosolic domains fold cotranslationally or whether they change conformation after synthesis. We used the CFTR as a model to examine this question.

CFTR, a member of the ABC transporter family, consists of 1480 amino acids that are organized into two membrane-spanning domains (MSD), two nucleotide binding domains (NBD), and a regulatory domain (R-domain) that is unique for CFTR (Riordan et al., 1989). The bulk of the protein (85%) is located in the cytosol, whereas the remainder resides in the ER membrane and the lumen (Figure 1A). CFTR is mainly expressed in epithelial cells, where it functions as a cAMP- and cGMP-dependent chloride channel at the plasma membrane (Riordan, 2005). Over 1000 different mutations mapped to the CFTR gene result in cystic fibrosis, the most common lethal genetic disorder among Caucasians.

Most data concerning CFTR folding were obtained by using pulse-chase analyses. Wild-type CFTR was reported to undergo an ATP-dependent posttranslational conformational change in NBD2 (Du et al., 2005; Lukacs et al., 1994) before it reaches its final folded and export-competent state. Pulse-chase studies also showed that CFTR is an inefficiently folding protein: ~50%–70% is degraded (Lukacs et al., 1994; Ward and Kopito, 1994) by the proteasome (Jensen et al., 1995; Ward et al., 1995). In lung epithelial cells that endogenously express CFTR, however, folding and maturation reach 100% efficiency (Varga et al., 2004). Although decisions concerning protein fate (ubiquitination) were found to occur during synthesis (Sato et al., 1998), no direct information concerning CFTR folding during synthesis is available.

To study the early folding pathway of CFTR in the ER membrane, we used in vitro translation in the presence of semipermeabilized cells in combination with limited proteolysis to determine protein conformation. We assessed which protease-resistant fragments relate to the CFTR domains and thereby established a powerful folding assay, not only to study CFTR but also other multispanning membrane proteins. By analyzing the folding of elongating CFTR nascent chains, we found

*Correspondence: i.braakman@chem.uu.nl
[3]Present address: Department of Molecular and Cell Biology, University of California, Berkeley, Berkeley, California 94720.
[4]Present address: Department of Cell Biology, University Medical Center Utrecht, Utrecht, The Netherlands.

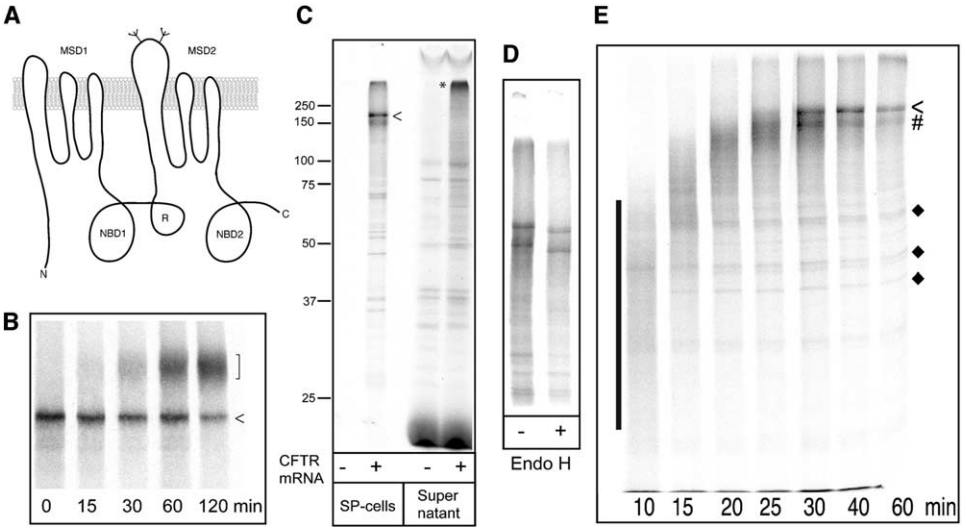

Figure 1. In Vivo versus In Vitro Synthesis of CFTR

(A) This schematic model of CFTR shows the domain architecture of the protein. It consists of two MSDs, each having six transmembrane segments, two NBDs, and an R-domain. N-glycans are present on the 4th extracellular loop.

(B) CFTR expressed in HeLa cells was radioactively pulse-labeled for 15 min and chased for the indicated times. CFTR was immunoprecipitated from the detergent cell lysates with polyclonal antiserum G449. The fast-migrating band represents the ER form (arrow), and the slower-migrating smear represents the complex glycosylated Golgi form (bracket).

(C) CFTR was translated for 60 min in the presence of semipermeabilized cells (SP-cells) as a source of ER membrane. Translocated full-length CFTR (<) and nontranslocated CFTR, mostly accumulated in aggregates (*), were obtained by separating cells from supernatant. In the absence of mRNA, no radiolabeled proteins were detectable on 12% SDS-PAGE that translocated into the SP-cells.

(D) To show that CFTR was translocated and inserted correctly into the ER membrane of SP-cells, we treated a 60 min sample (as in C) with endoglycosidase H.

(E) After 5 min prewarming the translation mix, we added ^{35}S-methionine and followed CFTR synthesis in the SP-cell system for 10–60 min. Analysis with 10% SDS-PAGE directly visualized CFTR nascent chain elongation with time. Full-length CFTR (<) appeared after 30 min of translation; "#" indicates CFTR translated from an alternative downstream start and "♦" indicates persistent unfinished nascent chains.

that this multidomain protein already acquired most of its structure cotranslationally.

Results

CFTR Synthesis in Intact and Semipermeable Cells

To study CFTR folding, a pulse-chase analysis, as shown in Figure 1B, is the general method of choice. HeLa cells expressing CFTR were pulse-labeled for 15 min and chased for the indicated times. CFTR was immunoprecipitated from the radiolabeled, nondenaturing detergent lysates by using a polyclonal antibody that specifically recognizes the R-domain and was analyzed by sodium dodecyl-sulfate-polyacrylamide gel electrophoresis (SDS-PAGE). The ER pool of CFTR (Figure 1B, arrowhead) reached the Golgi complex within 30–60 min, as judged by modification of the N-glycans by Golgi glycosyl transferases (Figure 1B, bracket). Although this conversion indicated that CFTR folded correctly and was released by the ER, this analysis does not allow discrimination between CFTR folding intermediates and its native ER export-competent conformation. To focus on ER folding events, we studied CFTR biosynthesis in vitro in the presence of semipermeabilized cells, an in vitro translation system in which CFTR is the only labeled protein present.

The plasma membrane of HT1080 cells was selectively permeabilized with digitonin. The washed out cytosol was replaced with rabbit reticulocyte lysate including all the components for in vitro translation (Wilson et al., 1995). After adding ^{35}S methionine, the translation mix was incubated at 30°C to synthesize radiolabeled CFTR. Figure 1C demonstrates that newly synthesized CFTR was found in the cell pellet, indicating proper translocation and insertion, into the ER membrane, of the semipermeable cells (SP-cells) as full-length protein (arrowhead). The protein contained the N-linked glycans on the 4th ER lumenal loop as shown by its increase in electrophoretic mobility upon glycan removal by endoglycosidase H treatment (Figure 1D). Not all newly synthesized CFTR folded properly. This pool accumulated as aggregates in the supernatant fraction (Figure 1C, asterisk), because degradation is largely inhibited by hemin present in the reticulocyte lysate (Xiong et al., 1999). When CFTR mRNA was omitted from the translation mix, labeled background proteins were detectable only in the supernatant fraction. All translocated polypeptides shown in Figure 1C therefore were CFTR-derived, demonstrating that CFTR can be analyzed directly by using SDS-PAGE. Because the SP-cell system contains no cytosol and hence does not support ER to Golgi traffic, we only focused on folding events in and at the ER membrane. We concluded that the multidomain protein CFTR translated efficiently in

our SP-cell system, allowing us to directly examine its early folding events at the ER membrane without the use of antibodies.

CFTR Nascent Chain Elongation

An advantage of the in vitro translation system is that it allows analysis of growing CFTR nascent chains to study CFTR folding from the very beginning. We prewarmed the translation mix for 5 min at 30°C and translated, in the presence of ^{35}S methionine, for 10, 15, 20, 25, 30, or 60 min. SDS-PAGE of samples translated for 10 min shows a heterogeneous nascent chain population, ranging from ~25–70 kDa, represented by the bar in Figure 1E. With time, these CFTR chains elongated, gradually decreased in electrophoretic mobility, and ended up as full-length CFTR of ~150 kDa after 30 min (Figure 1E, <). The band indicated by "#" is likely the result of an alternative start codon (Professor Philip Thomas, University of Texas, Southwestern Medical Center, TX, personal communication, and our unpublished data). During elongation, unfinished nascent chains appeared below the full-length protein, which remained present throughout the experiments (Figure 1E, ♦). These bands are not degradation products generated by residual proteasome activity because administration of MG132 during translation did not affect intensity or position of these bands. Addition of excess tRNA to the translation mix did not remove the unfinished nascent chains (data not shown). Whether they reflect intrinsic translation problems of CFTR synthesis is an interesting but unanswered question. Yet, this assay allows analysis of CFTR nascent chain elongation and folding.

Limited Proteolysis to Investigate CFTR Conformation

To investigate conformational changes during folding, we used limited proteolysis (Zhang et al., 1998) on in vitro synthesized CFTR in the presence of SP-cells. Immediately after 60 min of translation, the SP-cells containing CFTR were washed and solubilized in lysis buffer (see Experimental Procedures). CFTR was subjected to increasing concentrations of endoproteinase Glu-C, TPCK-trypsin, or proteinase K, which potentially cleave the protein at 93, 166, and 602 positions respectively. This means that we probed 861 out of 1480 amino acids in CFTR for conformation, which is close to 60%, spread out over the full-length of the molecule. Although the three proteases have very different specificities, they generated sets of fragments with similar electrophoretic mobilities, with the most comparable protease-resistant CFTR fragments indicated by asterisks in Figure 2A. This suggested that similarly folded structures can be detected irrespective of the protease used, indicating that our assay was done to saturation and that protease protection as we assayed it is a measure for CFTR folding. Although CFTR is a membrane protein, its solubilization in Triton X-100 prior to proteolysis did not affect protease susceptibility as shown in Figure S1 (see Figure S1 in the Supplemental Data available with this article online), which is in line with recent data of Lukacs and coworkers (Du et al., 2005).

To validate our conformational studies on CFTR translated in vitro in the SP-cell system, we compared its conformation with that of in vivo-translated CFTR. To this end, we immunoprecipitated both in vitro translated radiolabeled CFTR and in vivo radiolabeled CFTR from HeLa cells overexpressing the protein. Proteolysis was performed directly on immunopurified CFTR, before elution from the beads, and samples were analyzed by SDS-PAGE (Figure 2B). Although labeling intensities differed, we found that proteolytic patterns of in vitro-synthesized CFTR (Figure 2B, lanes 2, 5, and 8) were very similar to the proteolytic patterns of in vivo-synthesized CFTR (lanes 3, 6, and 9), indicating that the conformation of CFTR synthesized in SP-cells and in intact HeLa cells is the same. To assess whether immunoprecipitation influences the conformation of CFTR, we compared the proteolysis data of immunopurified CFTR and CFTR that was immediately treated with proteases after translation (lanes 1, 4, and 7). Although these proteolytic patterns were very similar, minor differences arose, probably from the footprint of the polyclonal antiserum on CFTR.

To confirm that our folding assay is conformation sensitive, we examined CFTR Δ650–830 (lacking residues 650–830 that mostly comprise the R-domain), which misfolds and is retained in the ER (Vankeerberghen et al., 1999). Treatment of CFTR Δ650–830 with proteinase K resulted in a strikingly different proteolytic pattern (Figure 2C, lanes 7–11) than that of wild-type protein (Figure 2C, lanes 2–5), having more smear and almost no discrete protease-resistant fragments. We concluded that CFTR Δ650–830 is completely misfolded, because the usually resistant MSD1 fragments (Figure 2C, lanes 5 and 11, double arrowheads; their identification will be shown below) became protease sensitive, even though the mutant's ER targeting was unaffected as determined by EndoH treatment (data not shown).

Because CFTR needs ATP for folding (Lukacs et al., 1994), we used ATP depletion to confirm that our assay indeed probes for CFTR conformation. After 60 min of translation, we stopped CFTR synthesis and folding by immediate ATP depletion using either apyrase or hexokinase and glucose. CFTR aggregated upon apyrase treatment, as shown by high molecular weight material at the top of the separation and stacking gels (Figure 2D, lane 2, brackets 1 and 2, respectively), whereas hexokinase treatment did not result in CFTR aggregation (Figure 2D, lane 3). To examine CFTR's folded state after apyrase treatment, we performed limited proteolysis with TPCK-trypsin (Figure 2D, lanes 4–12) or proteinase K (Figure 2D, lanes 13–21). Apyrase treatment affected the CFTR proteolysis patterns from both proteases, when compared to untreated and hexokinase-treated samples (Figure 2D, asterisks in lanes 8 and 17). We concluded that ATP depletion with apyrase resulted in CFTR misfolding, which we detected in our assay. Altogether these results validate our proteolysis assay as a measure for CFTR folding and conformation in semipermeabilized cells, which was confirmed further by the subtle changes we detected in two CF patient-related mutants, CFTR ΔF508 and CFTR P205S (our unpublished data).

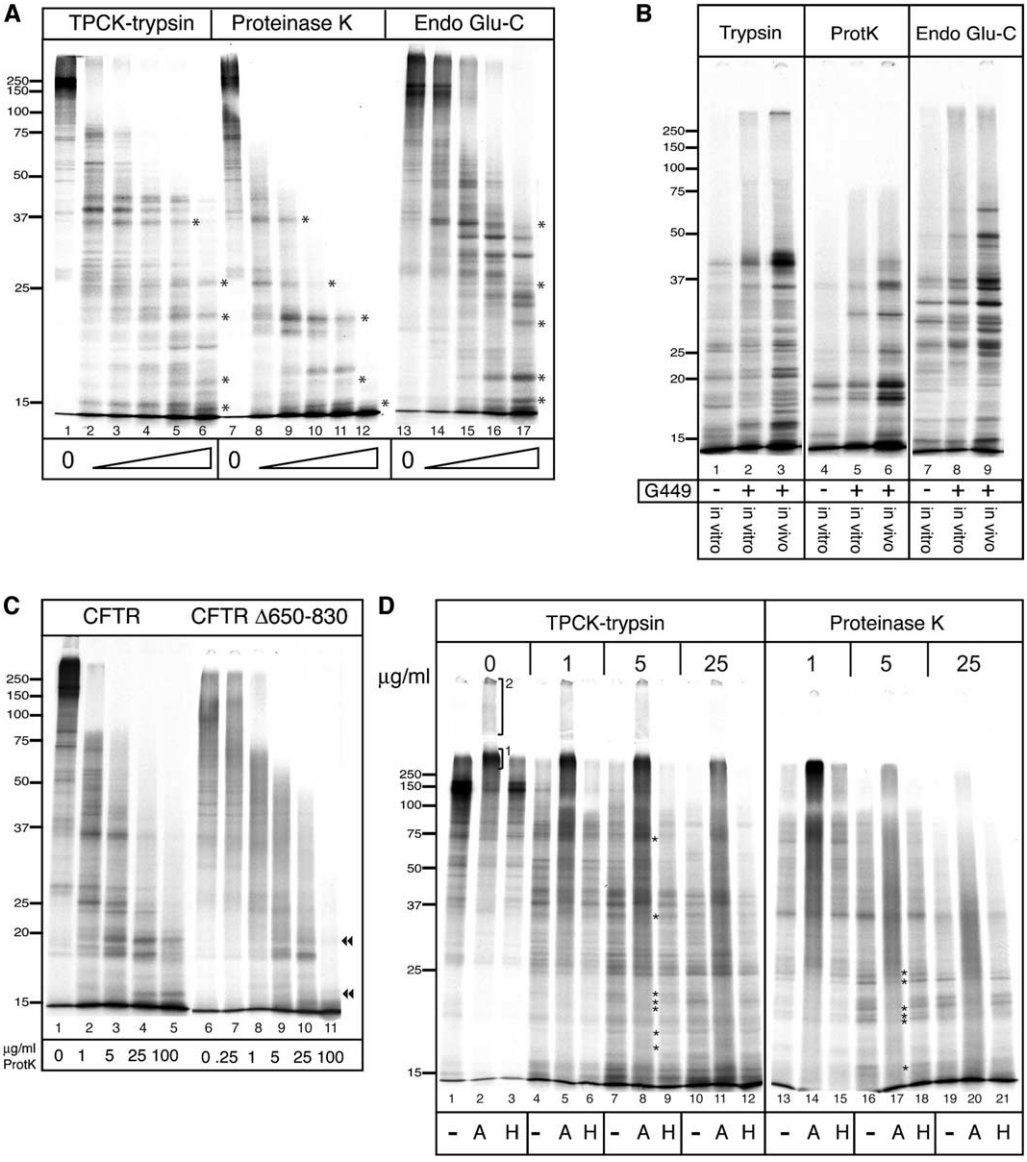

Figure 2. Limited Proteolysis to Study CFTR Conformation

(A) CFTR translated for 60 min was solubilized in lysis buffer and aliquoted. Increasing concentrations of TPCK-trypsin (1, 2.5, 5, 10, and 50 μg/ml), proteinase K (2.5, 10, 50, 100, and 500 μg/ml), or endoproteinase Glu-C (5, 25, 100, and 500 μg/ml) were added to determine protease susceptibility of CFTR. The resulting digests were analyzed using 12% SDS-PAGE. The asterisks indicate protease-resistant bands with similar electrophoretic mobility.

(B) CFTR expressed in HeLa cells was pulse-labeled for 15 min and in parallel CFTR was translated for 60 min in the presence of SP-cells to compare protease susceptibility of in vivo and in vitro synthesized protein, respectively. When indicated, CFTR was immunoprecipitated with the R-domain specific antibody G449 for 3 hr prior to proteolysis with 25 μg/ml TPCK-trypsin, proteinase K, or 100 μg/ml endoproteinase Glu-C. The proteolytic patterns were analyzed as in (A).

(C) Wild-type and CFTR Δ650–830 were translated in vitro for 60 min, treated with proteinase K after lysis, and analyzed as in (A). Double arrowheads mark examples of conformational differences.

(D) After 60 min, CFTR synthesis and folding were immediately stopped by depleting ATP with either apyrase (A) or hexokinase and glucose (H). After lysis, the conformation was probed using limited TPCK-trypsin or proteinase K proteolysis and analyzed as in (A). Brackets indicate CFTR aggregates and asterisks denote clear differences in protease resistance.

Identification of the Protease-Resistant Fragments

The complex proteolytic patterns of wild-type CFTR consisted of many bands with unknown identity. To identify protease-resistant fragments, we used CFTR molecules that were C-terminally truncated after MSD1 (N-MSD1, 1–394), NBD1 (N-NBD1, 1–642), R-domain, (N-R, 1–837), or MSD2 (N-MSD2, 1–1164), as shown in Figure 3A. The addition of a domain at the C terminus will add protease-resistant fragments specific for that domain, and/or it will change fragments of preceding

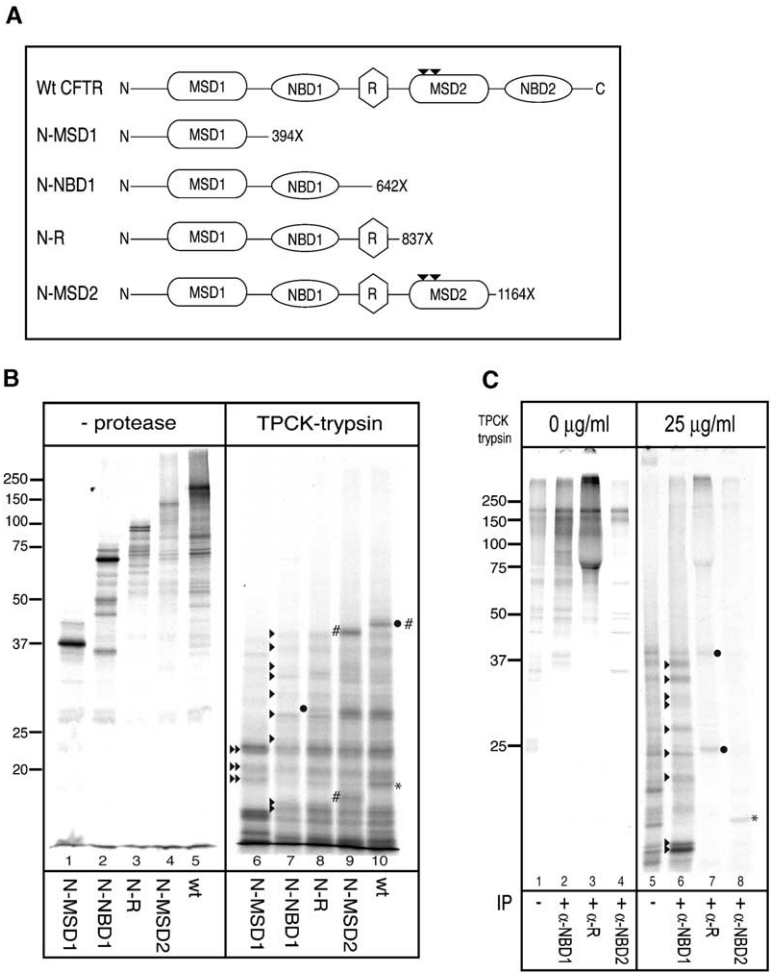

Figure 3. Identification of the Protease-Resistant Bands

(A) A schematic representation of the C-terminal CFTR truncations used in this study. (B) Wild-type CFTR and the C-terminal CFTR truncations were in vitro translated in the presence of SP-cells for 30 min (N-MSD1, N-NBD1, N-R) or 60 min (N-MSD2, wild-type CFTR) (left). After translation, all CFTR truncations were solubilized and subjected to digestion with 25 μg/ml TPCK-trypsin (right). The proteolytic pattern was analyzed by 12% SDS-PAGE. Protease-resistant fragments of wild-type CFTR were annotated and marked as follows: ▶▶, MSD1; ▶, NBD1; •, R-domain; #, MSD2; and *, NBD2. (C) Both in vitro translated full-length CFTR and the total proteolytic digest shown in (B) were immunoisolated using antibodies directed against NBD1 (L12B4), R-domain (G449), and NBD2 (M3A7). The precipitated material was loaded next to the input material (total proteolytic digest) as shown in lanes 1 and 5 and separated with 12% SDS-PAGE.

domain(s) that are connected to or affected by the added domain.

The shorter, truncated forms N-MSD1, N-NBD1, and N-R were translated for 30 min, and N-MSD2 and wild-type CFTR were translated for 60 min (Figure 3B). All CFTR truncations then were treated with 1, 5, 25, or 100 μg/ml TPCK-trypsin, proteinase K, or 5, 25, 100, or 500 μg/ml endoproteinase Glu-C. Digestion of full-length and truncated CFTR molecules with 25 μg/ml TPCK-treated trypsin showed a relatively straightforward proteolytic pattern (Figure 3B), which allowed identification of many bands in the full-length CFTR digestion pattern. Fragments already present in the N-MSD1 construct remained present in the longer constructs (Figure 3B, ▶▶), indicating that MSD1 in the full-length protein acquired protease-resistance at the moment it had been synthesized (Figure 3B, lanes 6–10). The same was true for fragments appearing upon addition of NBD1 (▶), the R-domain (•), MSD2 (#), and NBD2 (*) as marked in Figure 3B. Treatments with the other proteases are shown in Figure S2.

By using antibodies raised against NBD1 (L12B4), the R-domain (G449), and NBD2 (M3A7), we confirmed the identity of many protease-resistant fragments by selectively immunoprecipitating them from the total proteolytic digest. Identified NBD1, R-domain, and NBD2-related fragments are marked as follows: (▶) for NBD1 fragments (Figure 3C, lane 6), (•) for R-domain fragments (Figure 3C, lane 7), and (*) for NBD2 fragments (Figure 3C, lane 8). Although the NBD1 antibody precipitated many fragments (Figure 3C, lane 6), which was reported before (Du et al., 2005; Zhang et al., 1998), all these bands related to NBD1 (Figure 3B, compare lanes 6 and 7); protease-resistant fragments from CFTR truncated after MSD1 were not precipitated by the NBD1-specific antibody (Figure S3). The antibodies against the R-domain and NBD2 precipitated fewer fragments that did not overlap with the NBD1-related fragments, emphasizing the specificity of all the antibodies used. The lower R-domain fragment of ~25 kDa clearly became resistant in the N-R truncation (compare Figure 3B, lane 8 with Figure 3C, lane 7). The R-domain fragment of ~42 kDa, however, was found only when the MSD2 domain was added to the construct (Figure 3B, lane 10): part of the R-domain apparently forms a protease-resistant structure with MSD2 (unpublished data). These results show that almost all protease-resistant fragments can be identified by using comparative pro-

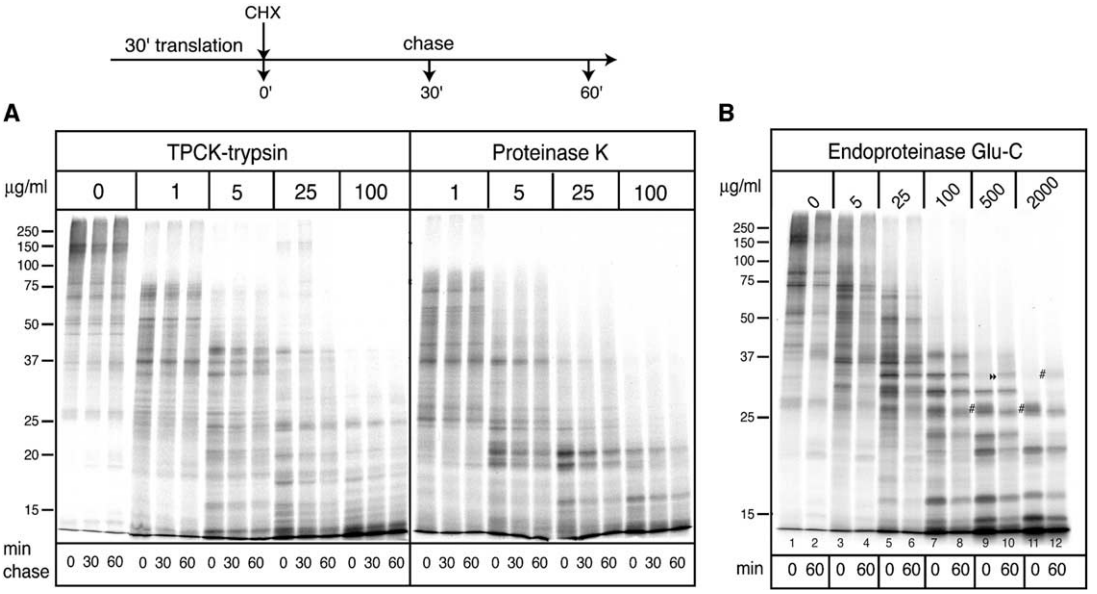

Figure 4. Posttranslational Changes of In Vitro-Synthesized CFTR

(A) When CFTR reached its full-length form after 30 min of translation, 5 mM cycloheximide (CHX) was added to stop nascent chain elongation. After the indicated chase times, CFTR was subjected to increasing concentrations of TPCK-trypsin or proteinase K to determine the extent of posttranslational folding. Fragments were analyzed with 12% SDS-PAGE.

(B) As in 4A, using increasing endoproteinase Glu-C concentrations. The differences we found are marked as in Figures 3B and 3C: ▸▸, MSD1; #, MSD2.

teolytic studies on C-terminal CFTR truncations, as confirmed by selective immunoprecipitation of domain fragments. We concluded that the CFTR truncations folded into distinct protease-resistant structures independent of the absent C-terminal domains.

CFTR Hardly Folds Posttranslationally

To investigate posttranslational folding of CFTR, we translated the protein in vitro for 30 min, the time to synthesize CFTR (see Figure 1E), and chased for 0, 30, and 60 min in the presence of 5 mM cycloheximide to stop elongation of nascent chains. CFTR conformation was analyzed by limited proteolysis with TPCK-trypsin, proteinase K, or endoproteinase Glu-C. Remarkably, the proteolytic patterns generated by the proteases that cleave most frequently (TPCK-trypsin and proteinase K) did not change with time, suggesting that CFTR conformation does not change at all after synthesis (Figure 4A). Only in the two highest endoproteinase Glu-C concentrations (Figure 4B) did we find a small but clear change in the proteolytic patterns from 0 to 60 min chase, indicative of some posttranslational folding. A fuzzy, doublet-like band disappeared (Figure 4B, lane 9, #), and one fragment acquired more resistance to the protease (Figure 4B, lane 10, ▸▸). Identification using the C-terminal CFTR truncations (Figure S2) suggested that both MSD1 (Figure 4B, ▸▸) and MSD2 (Figure 4B, #) change conformation posttranslationally. Because the slight posttranslational folding of CFTR could only be uncovered with high concentrations of endoproteinase Glu-C and not with TPCK-trypsin and proteinase K, we concluded that in vitro CFTR had folded almost completely during synthesis, coincident with the insertion of its transmembrane helices into the ER membrane.

To confirm these results, we examined CFTR folding in intact cells, especially because the in vitro assay does not allow transport to the Golgi complex and plasma membrane and therefore precludes analysis of mature, fully functional forms of CFTR. CFTR was pulse-labeled for 15 min in HeLa cells (Figure 5A, arrowhead) and chased for up to 3 hr in the presence of cycloheximide to generate mostly fully matured CFTR molecules (Figure 5A, bracket). We then examined the in vivo folded state of CFTR at both time points using TPCK-trypsin and Proteinase K proteolysis, as done in Figure 2B. Although CFTR was allowed to fold for 3 hr, its conformation remained virtually identical (Figure 5B, compare lane 1 with lane 2, and lane 5 with lane 6). Only a single protease-resistant band of ~42 kDa disappeared (Figure 5B, lanes 2 and 6, indicated as "#"), and a smear appeared instead (Figure 5B, lanes 2 and 6, bracket). These posttranslational changes, however, were attributed to modification of CFTR's N-glycans by the Golgi complex, because inhibition of ER to Golgi transport by brefeldin A (BFA) (Figure 5A) eliminated the differences (Figure 5B, lanes 3, 4, 7, and 8). The only posttranslational change left in vivo was detectable after TPCK-trypsin proteolysis; the band marked by "#" shifted down marginally during the chase (Figure 5B, compare lanes 3 and 4). This shift is most likely caused by glucose and mannose trimming of the two glycans, but we cannot exclude a small change in proteolytic sensitivity of MSD2. We concluded that, like in the in

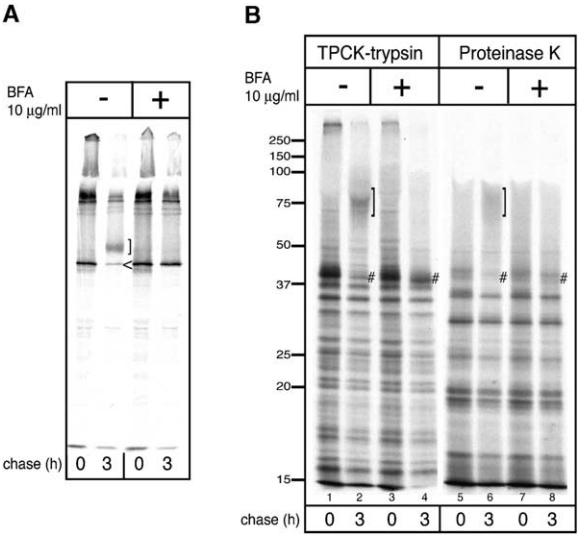

Figure 5. Posttranslational Changes of In Vivo-Synthesized CFTR

(A) HeLa cells transiently expressing CFTR were pulsed for 15 min and chased for 0 or 3 hr. CFTR was immunoprecipitated with G449 antiserum prior to analysis by 7.5% SDS-PAGE. Newly synthesized CFTR moved from ER (<) to cell surface via the Golgi complex where its N-glycans were modified (bracket). When cells were treated with 10 μg/ml BFA, transport from ER to Golgi was blocked. (B) Samples from Figure 5B were treated as in Figure 2B. The conformation of CFTR chased for 0 hr and 3 hr was compared using 25 μg/ml TPCK-trypsin or proteinase K proteolysis and analyzed by 12% SDS-PAGE. A minor difference in the proteolytic pattern is highlighted by "#."

vitro experiment shown in Figure 4, most of CFTR folding had finished at the end of its synthesis, implying a largely cotranslational process.

Cotranslational Folding of CFTR

Because folding of CFTR was almost completed at the end of translation, we set out to analyze the folding process during synthesis, i.e., on the growing nascent chain. We analyzed protease susceptibility of nascent chains translated for 10, 20, or 60 min (generated as in Figure 1E), of translated CFTR C-terminal truncations, and of CFTR translated for 30 min and chased for 0, 30, and 60 min in the presence of cycloheximide. For clarity, we only focus on endoproteinase Glu-C protease treatment (Figures 6A and 6B); additional data are shown in Figure S4. Noticeable are the striking similarities between the proteolytic patterns of the many different samples (Figures 6A and 6B), especially when comparing conformations of CFTR nascent chains (Figures 6A and 6B, lanes 1 and 2 in each) with full-length protein (Figures 6A and 6B, lanes 3 and 4 in each). Digestion, by endoproteinase Glu-C, of CFTR nascent chains synthesized for only 10 min already yielded many protease-resistant fragments (Figures 6A and 6B, lane 1 in each). These protease-resistance patterns were virtually identical to the proteolytic patterns of N-MSD1 (Figures 6A and 6B, lane 8 in each), indicating that after 10 min of synthesis, MSD1 structures obtained complete protease resistance (Figures 6A and 6B, lanes 1, ▶▶). When CFTR elongated further (Figures 6A and 6B, lane 2 in each), additional fragments appeared related to NBD1 or the R-domain (•▶) and MSD2 (#), making the proteolytic pattern almost identical to that of full-length CFTR (Figures 6A and 6B lanes 3 and 4 in each). Increasing the protease concentration not only showed the same results but also demonstrated that structures within early CFTR nascent chains were as protease resistant as full-length CFTR translated for 60 min (Figure 6B).

Although the proteolytic patterns of CFTR nascent chains generated with TPCK-trypsin and proteinase K were more smeared, the trend that conformation of CFTR nascent chains (20 min of translation) was virtually identical to that of full-length CFTR remained evident (Figure S4). Limited proteolysis of the CFTR truncations also demonstrated that N-terminal domains folded into well-defined, protease-resistant structures independent of C-terminal parts (Figures 3, 6A, and 6B and Figure S2). We conclude that CFTR folds almost completely during synthesis in a modular manner, domain by domain.

Discussion

In this study, we focused on early folding of the multimembrane-spanning CFTR protein, analyzed both during and after synthesis, separating cotranslational from posttranslational events. We found that all CFTR domains already reach a protease-resistant structure during nascent chain elongation, which strongly suggests a predominantly cotranslational mode of folding.

We combined limited proteolysis with in vitro translation in semipermeabilized cells to examine folding of CFTR. All three proteases used in this study showed similar results, indicating that our assay had reached saturation. For a number of reasons this is the best available assay for early folding of a large protein. First, CFTR is the only labeled protein in the SP-cell system, and methionines and cysteines are evenly distributed along the length of the molecule. All CFTR domains are therefore represented in our proteolytic digestion patterns, without a need for antibodies. Second, the assay allows detection of radiolabeled growing nascent chains at different stages of synthesis and therefore explores cotranslational folding. Third, by using three different proteases with nonoverlapping amino acid specificity, we probed 861 out of the 1480 amino acids (60% of the protein sequence) for conformation. This is in stark contrast to conformation-specific antibodies that usually only recognize small epitopes. Fourth, because we related protease-resistant fragments to CFTR domain(s), CFTR folding was examined domain by domain. Last, we found that the protease-resistant fragment patterns of in vitro- and in vivo-synthesized CFTR were virtually identical, demonstrating that CFTR folding in vitro in the semipermeabilized cells was very similar to its folding in intact cells.

We confirmed the conformation sensitivity of our folding assay by inducing CFTR misfolding through

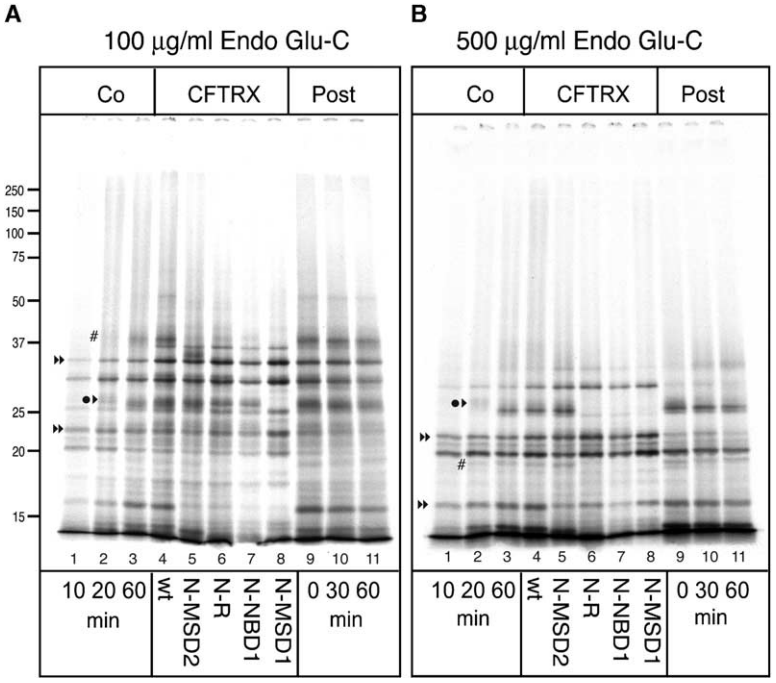

Figure 6. Folding during Nascent Chain Elongation of CFTR

(A) Nascent chains were synthesized for 10, 20, or 60 min as in Figure 1E and treated with 100 μg/ml endoproteinase Glu-C. All translated CFTR truncations and wild-type CFTR, labeled and chased as in Figure 5, were subjected to the same protease concentration and analyzed using 12% SDS-PAGE. Protease-resistant fragments are indicated as follows: ▸▸, MSD1; ▸, NBD1; •, R-domain; #, MSD2.

(B) Same as for 6A but with 500 μg/ml endoproteinase Glu-C.

either ATP depletion or deletion of amino acids 650–835, which mostly comprises the R-domain. We found that ATP depletion by apyrase had a drastic effect on CFTR structure, whereas ATP depletion by hexokinase and glucose did not. Apyrase can convert ATP all the way down to inorganic phosphate (Taussky and Shorr, 1953; Traverso-Cori et al., 1965), whereas hexokinase converts ATP to ADP. CFTR structure and function is likely to be affected directly because NBD domains bind ATP or ADP (Aleksandrov et al., 2001; Vergani et al., 2005). A need for ATP or ADP could also arise from the molecular chaperone Hsp70 involved in CFTR folding (Meacham et al., 1999), which needs the ATP/ADP cycle for efficient substrate binding and release (Bukau and Horwich, 1998). ADP generated by hexokinase will strengthen binding of Hsp70 to CFTR and maintain its solubility during folding. Without bound nucleotide, Hsp70 is likely to release and thereby induce CFTR aggregation. We found the same differential effects of apyrase and hexokinase on influenza hemagglutinin folding (M.C. Maggioni, I.M. Liscaljet, and I.B., unpublished data), where apyrase mimicked the phenotype of ATP depletion in intact cells (Braakman et al., 1992).

We made several observations that demonstrated a predominately cotranslational folding process for newly synthesized CFTR. The first and clearest evidence was found by directly examining the protease susceptibility of growing CFTR nascent chains. We found striking similarities in nascent chains of all lengths during elongation, including the first full-length forms of CFTR (Figure 6 and Figure S4). All folded and protease-resistant structures in the complete molecule already formed cotranslationally. Second, both in vitro and in vivo, we showed that CFTR did not show extensive posttranslational folding. Only upon proteolysis using endoproteinase Glu-C, which cleaves downstream of exposed glutamate residues in CFTR, did we find a posttranslational change in the proteolytic pattern, which related to MSD1 and MSD2. In intact cells, after a 3 hr chase that had allowed most CFTR molecules to pass the ER quality control, we found a small change that most likely was due to modification of the two N-glycans attached to MSD2. Third, we supplied evidence that cotranslational folding of CFTR is possible. Each truncated CFTR molecule yielded a proteolytic map with protease-resistant fragments similar to the fragments found in wild-type CFTR protein (Figure 3B and Figure S2), implying that the different C-terminal truncation constructs folded into wild-type-like structures. The folding of domains one by one and largely independent of C-terminal parts supports cotranslational folding. Expression of two CFTR half-molecules in *trans*, consisting of amino acids 1–837 and amino acids 837–1480, was shown before to yield functional CFTR at the cell surface (Ostedgaard et al., 1997). Intriguingly, the amino-terminal portion of CFTR alone (residues 1–836) already forms a regulated chloride channel, which is more stable than wild-type CFTR (Meacham et al., 1999; Sheppard et al., 1994).

Cotranslational folding is a recognized and unique feature of eukaryotic cells to improve folding efficiency and to reduce aggregation of soluble eukaryotic multidomain proteins (Netzer and Hartl, 1997). Our data show that this scenario also applies to CFTR. Formation of secondary structure elements can already occur inside the ribosomal tunnel and near the tunnel exit (Gilbert et al., 2004; Woolhead et al., 2004). Upon arrival at the translocon, α-helical transmembrane (TM) segments are ready for insertion into the bilayer, allowing cotranslational folding of the MSD domains. Most surprising was our finding that the large bulk of cytosolic CFTR domains folded during synthesis as well. An ad-

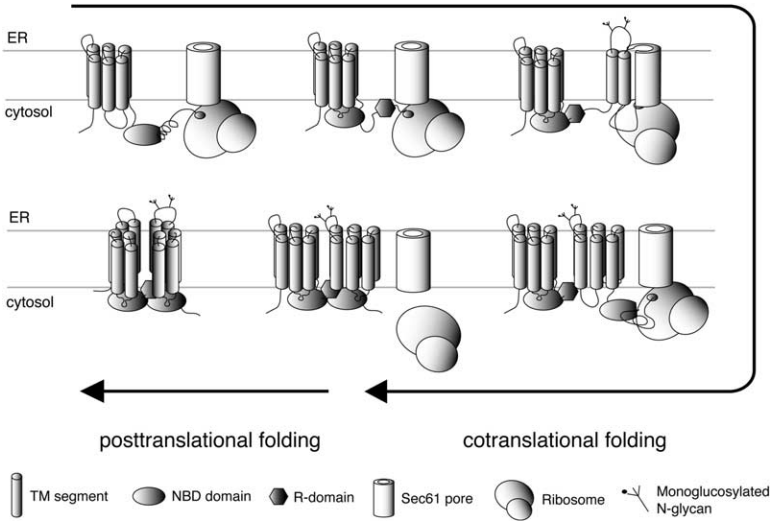

Figure 7. Model of CFTR Folding

This model describes the largely cotranslational folding pathway of CFTR that we propose from our experimental data. The CFTR domains fold sequentially in order of appearance and immediately interact with upstream domains. This requires crucial coordination by the ribosome and the Sec61 translocon. The only posttranslational folding we found involves both MSD domains, perhaps via denser packing of their transmembrane segments.

ditional factor supporting the cotranslational nature and efficiency of folding perhaps is the relatively low translation rate of CFTR, ~2.7 aa/sec (Ward and Kopito, 1994), compared to an average synthesis rate of ~4–5 aa/sec for other proteins (Braakman et al., 1991, and references therein). Whether this is merely a consequence of the size of CFTR or an effect of mutual regulation of folding and translation remains to be elucidated.

Based on our data, we propose a model, depicted in Figure 7, in which individual CFTR modules first fold fast and independently, after which they rapidly interact with a preceding domain cotranslationally to generate a more stable fold, as recently postulated for MSD1 and NBD1 (Thibodeau et al., 2005). This means that most of CFTR folding is over by the time of nascent chain termination. Still, full-length CFTR molecules on average reside in the ER longer than their synthesis time (see Figure 1B), suggesting additional conformational maturation steps are possible before exit. The only posttranslational folding we found was related to MSD1 and MSD2, possibly because of increasing compactness and interaction with each other (see Figure 7), reported before for P-Glycoprotein, a CFTR homolog (Loo and Clarke, 1998). CFTR MSD1 and MSD2 function in *trans* when expressed as separate proteins in vivo (Ostedgaard et al., 1997), and TM6 of MSD1 interacts with TM8 (Cotten and Welsh, 1999) and TM12 (Chen et al., 2004) of MSD2.

Lukacs and coworkers recently found that CFTR indeed folded cotranslationally to some extent but with posttranslational folding of NBD2 (Du et al., 2005). These authors, however, used different approaches by analyzing the folded state of only the NBD1 and NBD2 domains, using antibodies to detect proteolytic fragments, whereas we examined every single CFTR domain and fragment. In addition, the extent of cotranslational versus posttranslational folding was determined by ATP depletion, which is likely to result in CFTR misfolding and extensive aggregation as we showed here (Figure 2D); and CFTR was isolated from microsomes, perhaps allowing residual interaction with other proteins.

Our data do not exclude posttranslational conformational changes of CFTR due to associations with other polypeptide chains. Whether or not CFTR dimerizes is still a controversial issue. It does interact with many other ion channels and exchangers at the plasma membrane as a large hetero-multimeric complex responsible for conductance (Naren et al., 2003; Schwiebert et al., 1999). The Sulphonylurea receptor (Sur1A), a close family member of CFTR, forms a hetero-multimeric complex in the ER, which is a prerequisite for ER export (Schwappach et al., 2000). Analogous to Sur1A, the absence of partner proteins already in the ER may explain the inefficient folding of CFTR, mostly reported in CHO and BHK cells (with 50%–70% being degraded) (Lukacs et al., 1994; Ward and Kopito, 1994), and the 100% efficient maturation of CFTR in endogenously expressing lung and airway epithelial cells (Varga et al., 2004). Our assays in intact HeLa cells (Figures 1B and 5A) did not show degradation either, which underscores the sensitivity of CFTR degradation to cellular conditions and explains apparent discrepancies between our studies and those of others.

In summary, we found that in contrast to many large eukaryotic proteins, CFTR folded mostly during translation, translocation, and insertion of the protein into the ER membrane. The orchestrated vectorial folding of CFTR from N to C terminus, coupled with slow translation and translocation, may well facilitate efficient folding of this multidomain protein. Careful and detailed analysis of CFTR during nascent chain elongation, as we present here, will be needed to elucidate more of the CFTR folding process.

Experimental Procedures

Cell Lines and Medium

The human fibrosarcoma cell line HT1080 (American Type Culture Collection [ATCC] number CCL-12011) was maintained in Dulbecco's modified Eagle's medium (DMEM) supplemented with 8% fetal calf serum (FCS), 100 U/ml penicillin and streptomycin, and 2 mM GlutamaxI. The human cervical carcinoma cell line HeLa (ATCC number CCL-2) was maintained in MEM supplemented with 10% FCS, 100 U/ml penicillin and streptomycin, 2 mM GlutamaxI, and nonessential amino acids. All cells were cultured in humidified in-

cubators at 37°C under 5% CO_2. All cell culture media and reagents were obtained from Invitrogen.

Antibodies and Reagents

All proteases were purchased from Sigma. The G449 polyclonal antibody against the R-domain was kindly provided by Dr. Angus Nairn (Picciotto et al., 1992). The monoclonal antibodies L12B4 and M3A7 directed against NBD1 and NBD2, respectively, were purchased from Chemicon (Kartner et al., 1992).

CFTR Truncation Constructs

All C-terminal CFTR truncations were constructed with PCR amplification by introducing stop codons at the appropriate positions in the CFTR cDNA that was kindly provided by Dr. R.A. Frizzell. The primer combinations that were used are described in the Supplemental Data. The resulting CFTR truncation constructs pBS CFTR 394X (N-MSD1), pBS CFTR 642X (N-NBD1), pBS CFTR 837X (N-R), and pBS CFTR 1164X (N-MSD2) were sequence verified. All primers were purchased from Isogen and all cloning enzymes were purchased from New England Biolabs.

In Vitro Translation in the Presence of Semipermeabilized Cells

To in vitro translate and translocate proteins into the ER of digitonin-permeabilized HT1080 cells, the washed-out cytosol was replaced by rabbit reticulocyte lysate (Flexi Rabbit Reticulocyte Lysate System, Promega), mRNA of the protein of interest, and ^{35}S methionine/cysteine (10 μCi/μl Revidue PRO-MIX L-[^{35}S]; Amersham Biosciences) (Wilson et al., 1995). After incubation at 30°C, the reactions were stopped by adding ice-cold KHM buffer (110 mM KOAc, 20 mM HEPES [pH 7.2], 2 mM MgOAc) containing 1 mM cycloheximide. The 10,000 × g pellet fraction containing the SP cells was dissolved in KHM containing 1% Triton X-100, cleared by centrifugation, and was resuspended in Laemmli sample buffer. Before analysis by SDS-PAGE, samples were incubated for 10 min at 37°C. Detailed protocols can be found in the Supplemental Data.

ATP Depletion

ATP was depleted via conversion to ADP by adding 0.68 U/ml hexokinase (Roche) and 2 mM D-glucose to the translation mix in KHM buffer containing 1 mM cycloheximide and incubating at room temperature for 5 min. ATP was depleted and converted to AMP and free phosphate by adding 50 U/ml apyrase (Sigma) in KHM buffer containing 1 mM cycloheximide and incubating for 10 min at 37°C. Depletion of ATP was confirmed with a luciferase-luciferin ATP assay.

Limited Proteolysis

Immediately after translation, the SP cells were lysed in KHM buffer containing 1% Triton X-100. Protease susceptibility of CFTR was determined using a range of protease concentrations. After exactly 15 min of incubating on ice, 2.5 mM phenylmethylsulfonyl-fluoride (PMSF) was added before resuspending the digest in 2× Laemmli buffer. TPCK-trypsin was inhibited by adding a 5-fold excess of soybean trypsin inhibitor (SBTI). Either the obtained proteolytic digests were analyzed directly using 12% SDS-PAGE or fragments were immunoprecipitated from total proteolytic digest.

Endoglycosidase H Treatment

After translation, the semipermeabilized cell pellets containing radiolabeled CFTR were dissolved in 10 μl NaAc (pH 5.4) and 0.2% SDS and incubated for 10 min at 37°C. Then, 10 μl NaAc (pH 5.4) containing 1 mM PMSF, 10 μg/ml each of chymostatin, leupeptin, antipain, and pepstatin, 1% Triton X-100 (to quench the SDS), and 0.0025 U endoglycosidase H (Roche) was added and incubated for 1.5 hr at 37°C. The reaction was stopped by adding 2× Laemmli buffer, and the samples were analyzed with 7.5% SDS-PAGE.

Pulse-Chase Analysis and Immunoprecipitation

Subconfluent HeLa cells, grown in 6-cm dishes, were used 24 hr posttransfection for pulse-chase analysis as described before (Braakman et al., 1991). The cells were pulsed with 125 μCi/ml ^{35}S-methionine/cysteine for 15 min and chased with excess cold methionine/cysteine and 1 mM cycloheximide in HeLa medium at indicated times. The cells were lysed in ice-cold lysis buffer (20 mM MES, 50 mM Tris-Cl [pH 7.4], 100 mM NaCl, 1% Triton X-100, 1 mM PMSF, 10 μg/ml each of chymostatin, leupeptin, antipain, and pepstatin), nuclei were pelleted at 20,000 × g, and in most experiments CFTR was immunoprecipitated with polyclonal G499 serum. The samples were prepared for SDS-PAGE. For detailed immunoprecipitation protocols refer to the Supplemental Data online.

Supplemental Data

Supplemental Data including four figures and Supplemental Experimental Procedures are available online with this article at http://www.molecule.org/cgi/content/full/20/2/277/DC1/.

Acknowledgments

We thank Dr. Raymond Frizzell of the University of Pittsburg, PA for providing the pBS CFTR and pBS CFTR ΔF508 (pBQ 4.7) plasmids; Dr. Anne Vankeerberghen, University of Leuven, for the pcDNA3 CFTR and pcDNA3 CFTR-N1-C (Δ650–830) vectors; and Dr. Angus Nairn, Rockefeller University New York, for providing G449 and G450 polyclonal antisera directed against the CFTR R-domain. Drs. Marije Liscaljet, Adabella van der Zand, and Henk Tabak are acknowledged for their critical comments and valuable suggestions on the manuscript; Patrick Oei for the initial CFTR pulse-chase analysis; and Dr. Philip Thomas and all members of the Braakman lab for fruitful discussions. This work was supported by the Netherlands Science Organization, Medical branch, ZonMW.

Received: December 15, 2004
Revised: July 1, 2005
Accepted: September 6, 2005
Published: October 27, 2005

References

Alder, N.N., and Johnson, A.E. (2004). Cotranslational membrane protein biogenesis at the endoplasmic reticulum. J. Biol. Chem. *279*, 22787–22790.

Aleksandrov, L., Mengos, A., Chang, X., Aleksandrov, A., and Riordan, J.R. (2001). Differential interactions of nucleotides at the two nucleotide binding domains of the cystic fibrosis transmembrane conductance regulator. J. Biol. Chem. *276*, 12918–12923.

Bergman, L.W., and Kuehl, W.M. (1979). Formation of an intrachain disulfide bond on nascent immunoglobulin light chains. J. Biol. Chem. *254*, 8869–8876.

Braakman, I., Hoover-Litty, H., Wagner, K.R., and Helenius, A. (1991). Folding of influenza hemagglutinin in the endoplasmic reticulum. J. Cell Biol. *114*, 401–411.

Braakman, I., Helenius, J., and Helenius, A. (1992). Role of ATP and disulphide bonds during protein folding in the endoplasmic reticulum. Nature *356*, 260–262.

Bukau, B., and Horwich, A.L. (1998). The Hsp70 and Hsp60 chaperone machines. Cell *92*, 351–366.

Chen, E.Y., Bartlett, M.C., Loo, T.W., and Clarke, D.M. (2004). The DeltaF508 mutation disrupts packing of the transmembrane segments of the cystic fibrosis transmembrane conductance regulator. J. Biol. Chem. *279*, 39620–39627.

Chen, W., and Helenius, A. (2000). Role of ribosome and translocon complex during folding of influenza hemagglutinin in the endoplasmic reticulum of living cells. Mol. Biol. Cell *11*, 765–772.

Clemons, W.M., Jr., Menetret, J.F., Akey, C.W., and Rapoport, T.A. (2004). Structural insight into the protein translocation channel. Curr. Opin. Struct. Biol. *14*, 390–396.

Cotten, J.F., and Welsh, M.J. (1999). Cystic fibrosis-associated mutations at arginine 347 alter the pore architecture of CFTR. Evidence for disruption of a salt bridge. J. Biol. Chem. *274*, 5429–5435.

Du, K., Sharma, M., and Lukacs, G.L. (2005). The DeltaF508 cystic fibrosis mutation impairs domain-domain interactions and arrests post-translational folding of CFTR. Nat. Struct. Mol. Biol. *12*, 17–25.

Ellgaard, L., and Helenius, A. (2003). Quality control in the endoplasmic reticulum. Nat. Rev. Mol. Cell Biol. *4*, 181–191.

Gilbert, R.J., Fucini, P., Connell, S., Fuller, S.D., Nierhaus, K.H., Robinson, C.V., Dobson, C.M., and Stuart, D.I. (2004). Three-dimensional structures of translating ribosomes by Cryo-EM. Mol. Cell *14*, 57–66.

Jansens, A., van Duijn, E., and Braakman, I. (2002). Coordinated nonvectorial folding in a newly synthesized multidomain protein. Science *298*, 2401–2403.

Jensen, T.J., Loo, M.A., Pind, S., Williams, D.B., Goldberg, A.L., and Riordan, J.R. (1995). Multiple proteolytic systems, including the proteasome, contribute to CFTR processing. Cell *83*, 129–135.

Kartner, N., Augustinas, O., Jensen, T.J., Naismith, A.L., and Riordan, J.R. (1992). Mislocalization of delta F508 CFTR in cystic fibrosis sweat gland. Nat. Genet. *1*, 321–327.

Kim, P.S., Bole, D., and Arvan, P. (1992). Transient aggregation of nascent thyroglobulin in the endoplasmic reticulum: relationship to the molecular chaperone, BiP. J. Cell Biol. *118*, 541–549.

Kowarik, M., Kung, S., Martoglio, B., and Helenius, A. (2002). Protein folding during cotranslational translocation in the endoplasmic reticulum. Mol. Cell *10*, 769–778.

Loo, T.W., and Clarke, D.M. (1998). Superfolding of the partially unfolded core-glycosylated intermediate of human P-glycoprotein into the mature enzyme is promoted by substrate-induced transmembrane domain interactions. J. Biol. Chem. *273*, 14671–14674.

Lukacs, G.L., Mohamed, A., Kartner, N., Chang, X.B., Riordan, J.R., and Grinstein, S. (1994). Conformational maturation of CFTR but not its mutant counterpart (delta F508) occurs in the endoplasmic reticulum and requires ATP. EMBO J. *13*, 6076–6086.

Meacham, G.C., Lu, Z., King, S., Sorscher, E., Tousson, A., and Cyr, D.M. (1999). The Hdj-2/Hsc70 chaperone pair facilitates early steps in CFTR biogenesis. EMBO J. *18*, 1492–1505.

Morrison, T.G., Peeples, M.E., and McGinnes, L.W. (1987). Conformational change in a viral glycoprotein during maturation due to disulfide bond disruption. Proc. Natl. Acad. Sci. USA *84*, 1020–1024.

Naren, A.P., Cobb, B., Li, C., Roy, K., Nelson, D., Heda, G.D., Liao, J., Kirk, K.L., Sorscher, E.J., Hanrahan, J., and Clancy, J.P. (2003). A macromolecular complex of beta 2 adrenergic receptor, CFTR, and ezrin/radixin/moesin-binding phosphoprotein 50 is regulated by PKA. Proc. Natl. Acad. Sci. USA *100*, 342–346.

Netzer, W.J., and Hartl, F.U. (1997). Recombination of protein domains facilitated by co-translational folding in eukaryotes. Nature *388*, 343–349.

Ostedgaard, L.S., Rich, D.P., DeBerg, L.G., and Welsh, M.J. (1997). Association of domains within the cystic fibrosis transmembrane conductance regulator. Biochemistry *36*, 1287–1294.

Picciotto, M.R., Cohn, J.A., Bertuzzi, G., Greengard, P., and Nairn, A.C. (1992). Phosphorylation of the cystic fibrosis transmembrane conductance regulator. J. Biol. Chem. *267*, 12742–12752.

Riordan, J.R. (2005). Assembly of Functional CFTR Chloride Channels. Annu. Rev. Physiol. *67*, 701–718.

Riordan, J.R., Rommens, J.M., Kerem, B., Alon, N., Rozmahel, R., Grzelczak, Z., Zielenski, J., Lok, S., Plavsic, N., Chou, J.L., et al. (1989). Identification of the cystic fibrosis gene: cloning and characterization of complementary DNA. Science *245*, 1066–1073.

Sato, S., Ward, C.L., and Kopito, R.R. (1998). Cotranslational ubiquitination of cystic fibrosis transmembrane conductance regulator in vitro. J. Biol. Chem. *273*, 7189–7192.

Schwappach, B., Zerangue, N., Jan, Y.N., and Jan, L.Y. (2000). Molecular basis for K(ATP) assembly: transmembrane interactions mediate association of a K+ channel with an ABC transporter. Neuron *26*, 155–167.

Schwiebert, E.M., Benos, D.J., Egan, M.E., Stutts, M.J., and Guggino, W.B. (1999). CFTR is a conductance regulator as well as a chloride channel. Physiol. Rev. *79*, S145–S166.

Sheppard, D.N., Ostedgaard, L.S., Rich, D.P., and Welsh, M.J. (1994). The amino-terminal portion of CFTR forms a regulated Cl- channel. Cell *76*, 1091–1098.

Taussky, H.H., and Shorr, E. (1953). A microcolorimetric method for the determination of inorganic phosphorus. J. Biol. Chem. *202*, 675–685.

Thibodeau, P.H., Brautigam, C.A., Machius, M., and Thomas, P.J. (2005). Side chain and backbone contributions of Phe508 to CFTR folding. Nat. Struct. Mol. Biol. *12*, 10–16.

Traverso-Cori, A., Chaimovich, H., and Cori, O. (1965). Kinetic studies and properties of potato apyrase. Arch. Biochem. Biophys. *109*, 173–184.

Vankeerberghen, A., Lin, W., Jaspers, M., Cuppens, H., Nilius, B., and Cassiman, J.J. (1999). Functional characterization of the CFTR R domain using CFTR/MDR1 hybrid and deletion constructs. Biochemistry *38*, 14988–14998.

Varga, K., Jurkuvenaite, A., Wakefield, J., Hong, J.S., Guimbellot, J.S., Venglarik, C.J., Niraj, A., Mazur, M., Sorscher, E.J., Collawn, J.F., and Bebok, Z. (2004). Efficient intracellular processing of the endogenous cystic fibrosis transmembrane conductance regulator in epithelial cell lines. J. Biol. Chem. *279*, 22578–22584.

Vergani, P., Lockless, S.W., Nairn, A.C., and Gadsby, D.C. (2005). CFTR channel opening by ATP-driven tight dimerization of its nucleotide-binding domains. Nature *433*, 876–880.

Wallin, E., and von Heijne, G. (1998). Genome-wide analysis of integral membrane proteins from eubacterial, archaean, and eukaryotic organisms. Protein Sci. *7*, 1029–1038.

Ward, C.L., and Kopito, R.R. (1994). Intracellular turnover of cystic fibrosis transmembrane conductance regulator. Inefficient processing and rapid degradation of wild-type and mutant proteins. J. Biol. Chem. *269*, 25710–25718.

Ward, C.L., Omura, S., and Kopito, R.R. (1995). Degradation of CFTR by the ubiquitin-proteasome pathway. Cell *83*, 121–127.

Wilson, R., Allen, A.J., Oliver, J., Brookman, J.L., High, S., and Bulleid, N.J. (1995). The translocation, folding, assembly and redox-dependent degradation of secretory and membrane proteins in semi-permeabilized mammalian cells. Biochem. J. *307*, 679–687.

Woolhead, C.A., McCormick, P.J., and Johnson, A.E. (2004). Nascent membrane and secretory proteins differ in FRET-detected folding far inside the ribosome and in their exposure to ribosomal proteins. Cell *116*, 725–736.

Xiong, X., Chong, E., and Skach, W.R. (1999). Evidence that endoplasmic reticulum (ER)-associated degradation of cystic fibrosis transmembrane conductance regulator is linked to retrograde translocation from the ER membrane. J. Biol. Chem. *274*, 2616–2624.

Zhang, F., Kartner, N., and Lukacs, G.L. (1998). Limited proteolysis as a probe for arrested conformational maturation of delta F508 CFTR. Nat. Struct. Biol. *5*, 180–183.